

Anti-bullying Adaptive Cruise Control: A proactive right-of-way protection approach

Jia Hu, *Senior Member, IEEE*, Zhexi Lian, Haoran Wang, *Member, IEEE*, Zihan Zhang, Ruoxi Qian, Duo Li, Jaehyun (Jason) So, Junnian Zheng

Abstract— The current Adaptive Cruise Control (ACC) systems are vulnerable to “road bully” such as cut-ins. This paper proposed an Anti-bullying Adaptive Cruise Control (AACC) approach with proactive right-of-way protection ability. It bears the following features: i) with the enhanced capability of preventing bullying from cut-ins; ii) optimal but not unsafe; iii) adaptive to various driving styles of cut-in vehicles; iv) with real-time field implementation capability. The proposed approach can identify other road users’ driving styles online and conduct game-based motion planning for right-of-way protection. A detailed investigation of the simulation results shows that the proposed approach can prevent bullying from cut-ins and be adaptive to different cut-in vehicles’ driving styles. The proposed approach is capable of enhancing travel efficiency by up to 29.55% under different cut-in gaps and can strengthen driving safety compared with the current ACC controller. The proposed approach is flexible and robust against traffic congestion levels. It can improve mobility by up to 11.93% and robustness by 8.74% in traffic flow. Furthermore, the proposed approach can support real-time field implementation by ensuring less than 50 milliseconds computation time.

I. INTRODUCTION

Adaptive Cruise Control (ACC) system is one of the most broadly commercialized driving assistance functions. Over 50% of newly sold vehicles have been equipped with ACC[1]. ACC systems can reduce drivers’ workload and improve driving safety [2][3]. **However, current ACC systems significantly suffer from “road bully”, such as vehicle cut-ins.** When faced with such situations, current ACC systems often have to yield to the cut-in vehicle, frequently resulting in the loss of right-of-way. The loss of right-of-way may cause mobility reduction and rise in safety risks. Due to the vulnerable right-of-way, current ACC systems are frequently taken over by drivers [4]. **Hence, it is in great need to develop an anti-bullying ACC system with enhanced right-of-way protection capability.**

To prevent cut-ins from other vehicles, the earliest anti-bullying ACC systems were developed using rule-based

approaches. This type of approach relied on hand-crafted rules to activate different safety-oriented precautions [5][6]. Each precaution was designed to address specific types of cut-in maneuvers [7][8][9]. However, rule-based approaches often fail to respond effectively to cut-in maneuvers that the ego vehicle has never met before. Given an illustrative example, if another vehicle suddenly cuts in at a very close distance, the ego vehicle cannot avoid a collision because no rules have been developed to respond to the urgent cut-in. This limitation results in poor right-of-way protection capability.

To effectively handle unexpected cut-in maneuvers using intelligent strategies, recent research has focused more on learning-based approaches [10][11][12]. These approaches continuously accumulate driving experience from a wide range of previously encountered cut-in maneuvers [13][14]. By imitating how human drivers respond to these maneuvers, such approaches improve their driving responses over time, becoming adaptive to a wide variety of cut-in scenarios. However, such approaches still have limitations. Firstly, learning-based approaches often lack interpretability and fail to account for vehicle dynamics. As a result, actions produced by such approaches may exceed vehicles’ operational capabilities and compromise safety [15]. Secondly, learning-based approaches cannot guarantee the global optimality of driving maneuvers. For instance, the actions produced by such approaches might prioritize immediate collision avoidance but fail to account for travel efficiency. This occurs because the actions are often heuristic approximations based on previous experiences with inherent randomness, rather than definitive global optimal maneuvers in real-time [16].

To enhance driving maneuvers’ safety and optimality, model-based approaches have been widely adopted in anti-bullying ACC systems. These approaches address multi-objective optimization problems under safety constraints, hence ensuring both safety and global optimality of driving maneuvers [17]. However, existing model-based approaches are typically conducted in a “prediction → optimization”

This paper is partially supported by XXX. (*Corresponding author: Haoran Wang*)

Jia Hu and Zhexi Lian are with Key Laboratory of Road and Traffic Engineering of the Ministry of Education, Tongji University, No.4800 Cao’an Road, Shanghai, China, 201804. (e-mail: hujia@tongji.edu.cn, zhexi_lian@tongji.edu.cn)

Haoran Wang is with Key Laboratory of Road and Traffic Engineering of the Ministry of Education, Tongji University, Shanghai 201804, China, and State Key Laboratory of Advanced Design and Manufacturing for Vehicle Body, Hunan University, Changsha, 410082, China (e-mail: wang_haoran@tongji.edu.cn).

Zihan Zhang is with Shanghai Motor Vehicle Inspection Certification and Tech Innovation Center Co., LTD, 68 South Yutian Road, Shanghai, P.R.China, 201805. (e-mail: zihanz02@smvic.com.cn)

Ruoxi Qian is with University College London, 25 Gordon Street, London, United Kingdom. (e-mail: ruoxi.qian.22@ucl.ac.uk)

Duo Li is with Department of Civil and Geospatial Engineering, Newcastle University, Newcastle upon Tyne NE1 7RU, UK. (e-mail: duoli0725@gmail.com)

Jaehyun So is with the Department of Transportation System Engineering, Ajou University, Suwon, Gyeonggi 16499, South Korea (e-mail: jso@ajou.ac.kr).

Junnian Zheng is with Hyperview Mobility (Shanghai) Co., Ltd. No.488 Anchi Rd, Shanghai, 201805, P.R.China. (e-mail: junnian.zheng@hongjingdrive.com)

fashion, which means predicting the cut-in vehicle's trajectory first and optimizing the ego vehicle's motion second. This operation fashion has three main limitations. **Firstly, model-based approaches rarely consider proactively discouraging cut-in maneuvers.** Instead, they merely react passively to the cut-ins [18][19][20]. That's because the motion optimization is constrained by the predicted cut-in vehicles' trajectories. Given an illustrative example, these approaches can only optimize collision avoidance maneuvers if the predicted trajectory indicates a cut-in. In contrast, a skilled human driver can consider cut-in vehicles' reactions and conduct proactively driving maneuvers (such as accelerating) to discourage potential cut-ins [21]. **Secondly, model-based approaches lack resilience against different driving styles of cut-in vehicles** [22][23][24][25]. For instance, without recognizing the highly aggressive nature of specific cut-in vehicles, these approaches may consider accelerating as the optimal driving maneuver. However, blindly accelerating may not only fail to prevent cut-ins but also introduce high safety risks. **Thirdly, model-based approaches lack consideration of real-time field implementation capability.** For the prediction process, real-time inference is time-consuming if not provided with a high-computing-power device [26][27][28][29]. For the optimization process, mixed-integer and nonlinear problems are also time-consuming [17][20]. Conducting prediction and optimization at the same time makes it impossible to achieve a control frequency exceeding 10 Hz. Hence, the practicality of the above approaches in real-world applications is limited. To this end, model-based approaches need to be improved.

To overcome the above limitations, this research proposed an Anti-bullying Adaptive Cruise Control (AACC) approach. It bears the following features:

- With the enhanced capability of preventing bullying from cut-ins.
- Optimal but not unsafe
- Adaptive to various driving styles of cut-in vehicles.
- With real-time field implementation capability.

The remainder of this paper is organized as follows. Section II describes the highlights of this study; Section III describes the methodology of the study; Section IV shows the experimental conditions and the evaluation results; Section V provides brief conclusions of the results.

II. HIGHLIGHT

A. Anti-bullying via proactive right-of-way protection

The main function of the proposed approach is to prevent "road bully" during the ACC maneuver. This anti-bullying function is achieved by proactively discouraging potential cut-in maneuvers from other vehicles. Specifically, this approach works by having the ego vehicle take actions to discourage other vehicles' cut-ins. For instance, the ego vehicle could accelerate to close the following gap when other vehicles attempt to cut in. This makes other vehicles feel that the gap is insufficient for a cut-in maneuver. Consequently, other vehicles' cut-in attempts are disrupted.

B. Optimal planning responding to cut-in vehicles' all reactions

The proposed approach can ensure optimal planning for

the ego vehicle. This approach integrates the other vehicle's reaction functions into the system dynamics of the ego vehicle's optimal planning. Thus, the ego vehicle could consider other vehicles' all possible reactions to find its optimal maneuver. For instance, although the ego vehicle accelerates to close the gap, other vehicles still have a high probability of squeezing into the gap. In this case, the ego-vehicle may make its optimal decisions to yield to the cut-ins.

C. Enabled to identify personalized driving styles of cut-in vehicles

The proposed approach can adapt to various driving styles of other vehicles. The proposed approach enables online identification of personalized driving styles of cut-in vehicles. Hence person-by-person countermeasure maneuvers could be planned in response to other vehicles' personalized driving styles. For instance, if the other vehicle behaves aggressively, the ego-vehicle would yield to mitigate potential risks. Conversely, if the other vehicle is hesitant, the ego-vehicle would accelerate to prevent cut-ins. Consequently, the proposed approach is flexible to the change of driving styles of cut-in vehicles.

D. With real-time computation efficiency

To improve the practicality of the proposed approach, a quadratic programming problem is formulated with linear constraints. This formulation ensures computational efficiency in the real-time field implementation.

III. METHODOLOGY

A. Scenario of interests

The scenario of interest is a freeway. As shown in Figure 1, the Ego Vehicle (EV) is an autonomous vehicle equipped with the proposed AACC system. It also has multiple sensors and a GPS device to collect information on its state and other vehicles' trajectory data. The Preceding Vehicle (PV) is the closest following target of EV. The cut-in vehicle (also named the Competing Vehicle, CV) in the adjacent lane tends to cut in the EV mandatorily. EV competes with CV for right-of-way. The primary goal of the proposed AACC approach is to protect bullying from mandatory cut-ins during adaptive cruising.

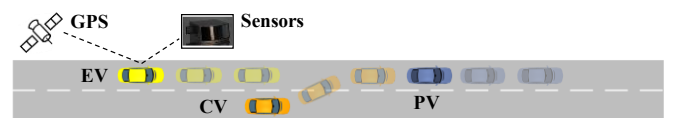


Figure 1 Scenario of interest.

B. System architecture

The AACC approach is formulated under the Partially Observable Markov Decision Process (POMDP) framework [30]. POMDP is a valid mathematical framework for decision-making under uncertainty. It is defined by the tuple $(\mathcal{S}, \mathcal{A}, \mathcal{O}, \mathcal{Z}, \mathcal{T}, \mathcal{R})$. \mathcal{S} is the state space. $\mathbf{u}_{EV} \in \mathcal{A}$ is the action space for EV. \mathcal{O} is the observation space which contains the observed physical state of vehicles, such as position, speed, and acceleration. \mathcal{Z} is the observation model. \mathcal{T} denotes the system state transition model (See Section III-C) and \mathcal{R} is the reward function (See Section III-E). In the proposed POMDP framework, CV has internal states β (See Section III-D) that reflect its driving style. EV cannot observe these internal states

directly. Therefore, EV maintains a belief \mathcal{B} as an estimate of the internal states β . The belief \mathcal{B} updates based on the observed history trajectory data of CV. This research solves the POMDP problem from an optimal control perspective. The detailed system structure of the proposed AACC approach is illustrated in Figure 2.

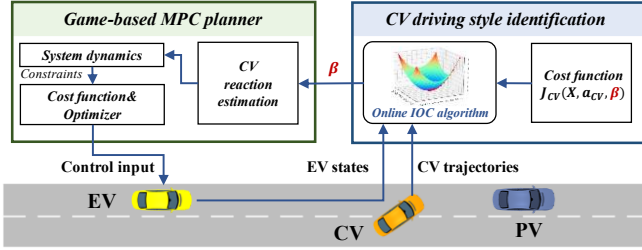


Figure 2 System structure.

- **CV individual driving style identification.** This module is to online identify CV's driving styles, in other words, estimating internal states β in the POMDP framework. Utilizing observations such as EV states and CV trajectories, this module would learn the longitudinal and lateral driving style parameters of CV and feed them into the downstream EV planning.

- **Game-based MPC Planner.** This module optimizes a person-by-person interdependent driving strategy for EV to protect right-of-way. The module inputs contain the internal states β and the current states of EV and CV. To embed CV's reaction, the EV's motion planning is formulated as a Game-based Model Predictive Control (GMPC) problem. The GMPC planner outputs commands as local control inputs of EV, with the consideration of CV's reaction. It enables the optimal driving maneuvers for EV in the competition with CV.

C. CV-EV interaction system dynamics

The CV-EV interaction system dynamics are modeled as the state transition model \mathcal{T} . Since CV conducts longitudinal and lateral coupled cut-in maneuvers and EV conducts longitudinal only maneuvers, the system state vector shall include the longitudinal and lateral state of CV and the longitudinal state of EV, defined as:

$$\mathbf{x} = (\Delta x, v_{EV}, v_{CV}, y_{CV}, \psi_{CV})^T \quad (1)$$

where Δx denotes the longitudinal distance between EV and CV; v_{EV} is the speed of EV; v_{CV} is the speed of CV; y_{CV} represents CV's lateral position and ψ_{CV} represents CV's yaw angle. As only EV is controlled, the control input of EV is defined as:

$$u_{EV} = a_{EV}, \quad u_{EV} \in \mathcal{A} \quad (2)$$

where a_{EV} denotes the acceleration of EV.

The CV-EV interaction system dynamics are modeled using the vehicle kinematic bicycle model [31]. The vehicle system is illustrated in Figure 3. φ is the angle of the current velocity of gravity center with respect to the longitudinal axis of the vehicle. For CV, both longitudinal and lateral kinematics need to be considered. The detailed formulation of the model is as follows:

$$\dot{x}_{CV} = v_{CV} \cos(\psi_{CV} + \varphi) \quad (3a)$$

$$y_{CV} = v_{CV} \sin(\psi_{CV} + \varphi) \quad (3b)$$

$$\dot{\psi}_{CV} = \frac{v_{CV}}{l_r} \sin \varphi \quad (3c)$$

$$v_{CV} = a_{CV} \quad (3d)$$

$$\varphi = \tan^{-1} \left(\frac{l_r}{l_r + l_f} \tan \delta_f \right) \quad (3e)$$

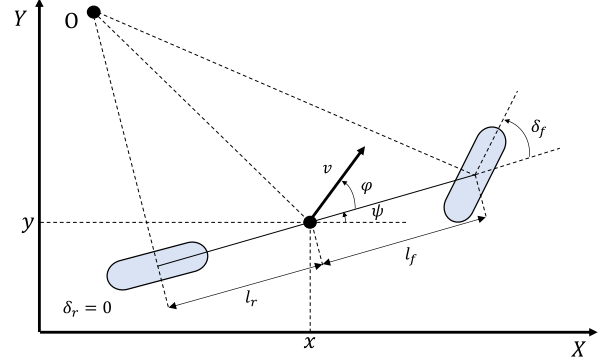


Figure 3 Kinematic bicycle model notation.

where l_r and l_f are distance between vehicle's gravity center and the rear and front axles respectively; δ_f denotes CV's front steering angle. For EV, only longitudinal kinematic need to be considered:

$$\dot{x}_{EV} = v_{EV} \quad (4a)$$

$$v_{EV} = a_{EV} \quad (4b)$$

Based on the small angle assumption of φ [32], the kinematic bicycle model, i.e., equation (3) is linearized. Then, the linear CV-EV interaction system dynamics (also known as the state transition model \mathcal{T}) integrating the kinematic models of both EV and CV could be derived as follows:

$$\dot{\mathbf{x}} = \mathbf{A}\mathbf{x} + \mathbf{B}u_{EV} + \mathbf{C}u_{CV} \quad (5)$$

where,

$$\mathbf{A} = \begin{bmatrix} 0 & 1 & -1 & 0 & 0 \\ 0 & 0 & 0 & 0 & 0 \\ 0 & 0 & 0 & 0 & 0 \\ 0 & 0 & 0 & 0 & v_{CV} \\ 0 & 0 & 0 & 0 & 0 \end{bmatrix} \quad (6a)$$

$$\mathbf{B} = \begin{bmatrix} 0 \\ 1 \\ 0 \\ 0 \\ 0 \end{bmatrix} \quad (6b)$$

$$\mathbf{C} = \begin{bmatrix} 0 & 0 \\ 0 & 0 \\ -1 & 0 \\ 0 & \frac{v_{CV}}{l_f + l_r} \\ 0 & \frac{v_{CV}}{l_f + l_r} \end{bmatrix} \quad (6c)$$

$$\mathbf{u}_{CV} = (a_{CV}, \delta_f)^T \quad (6d)$$

D. CV driving style identification

To identify the driving style of CV, a novel online inverse optimal control (IOC) algorithm is applied in this research [33]. Given the parametrized driving features (driving safety, travel efficiency, ride comfort, etc.), this algorithm can utilize the

individual trajectory data to recognize the driver's preference for these features thus learning the knowledge about CV's individual driving style.

1) Definition of CV's individual driving style β

This research defines β as weighting factors of CV's cost function:

$$J_{CV} = \frac{1}{2} \sum_{n=0}^{N-1} \left[\underbrace{\beta_1 (\Delta x_n - \Delta x_{des}^{CV})^2}_{\text{driving safety}} + \underbrace{\beta_2 (v_{CV,n} - v_{des}^{CV})^2}_{\text{driving efficiency}} + \underbrace{\beta_3 a_{CV,n}^2}_{\text{ride comfort}} + \underbrace{\beta_4 (y_{CV,n} - y_{des}^{CV})^2}_{\text{lane-changing request}} + \underbrace{\beta_5 \psi_{CV,n}^2}_{\text{motion smoothness}} \right] \quad (7a)$$

$$\beta = (\beta_1, \beta_2, \beta_3, \beta_4, \beta_5)^T \quad (7b)$$

where N denotes the optimization steps in the optimization horizon T and n denotes the current optimization step; Δx_{des}^{CV} represents the desired longitudinal safe distance of CV while v_{des}^{CV} represents the desired speed of CV; y_{des}^{CV} denotes the desired lateral position of CV. The first three terms in equation (7a) driving safety feature, driving efficiency feature, and ride comfort feature of CV. They are longitudinal driving features. The fourth term in equation (7a) denotes CV's lane-change requests. If CV is tended to cut in EV, y_{des}^{CV} denotes the y coordinate of the target lane centerline. The fifth term can reduce the change of yaw angle to ensure CV's motion smoothness. The last two terms are lateral driving features. The parameters $\beta_1, \beta_2, \beta_3, \beta_4, \beta_5$ determine the individual driving styles of CV as they can reflect CV's preference to different driving features. The equation (7a) can be further transformed to the following form:

$$J_{CV} = \frac{1}{2} \sum_{n=0}^{N-1} \begin{pmatrix} \beta_1 \\ \beta_2 \\ \beta_3 \end{pmatrix}^T \begin{pmatrix} (\Delta x_n - \Delta x_{des}^{CV})^2 \\ (v_{CV,n} - v_{des}^{CV})^2 \\ a_{CV,n}^2 \end{pmatrix} + \begin{pmatrix} \beta_4 \\ \beta_5 \end{pmatrix}^T \begin{pmatrix} (y_{CV,n} - y_{des}^{CV})^2 \\ \psi_{CV,n}^2 \end{pmatrix} \quad (8)$$

$$= \frac{1}{2} \sum_{n=0}^{N-1} \underbrace{\beta_{long}^T L_{long,n}(\mathbf{x}_{long,n}, a_{CV,n})}_{\text{longitudinal components}} + \frac{1}{2} \sum_{n=0}^{N-1} \underbrace{\beta_{lat}^T L_{lat,n}(\mathbf{x}_{lat,n})}_{\text{lateral components}} \quad (8)$$

$$\mathbf{x}_{long,n} = (\Delta x_n, v_{EV,n}, v_{CV,n})^T \quad (9a)$$

$$\mathbf{x}_{lat,n} = (y_{CV,n}, \psi_{CV,n})^T \quad (9b)$$

where β_{long} represents parameters reflecting longitudinal driving features, including $\beta_1, \beta_2, \beta_3$; β_{lat} represents CV's preference to lateral driving features, including β_4, β_5 ; $\mathbf{x}_{long,n}$ and $\mathbf{x}_{lat,n}$ contains the longitudinal and lateral components of system state \mathbf{x} at step n , respectively.

2) Algorithm formulation

The online IOC algorithm is formulated as follows. This research assumes that the action of CV follows an optimal control scheme and the cost function is equation (8). As the lateral and longitudinal movement of vehicles follows different movement modes, this research separately identifies the parameters β_{long} and β_{lat} using the same online IOC algorithm. Due to paper length limitations, this research takes β_{long} identification as an example to formulate the algorithm. Based on Pontryagin's Minimum Principle [34], the solution to the longitudinal components of equation (8) shall satisfy the following necessary conditions:

$$\lambda_n = \nabla_{\mathbf{x}_{long,n}} H_n(\mathbf{x}_{long,n}, a_{CV,n}, \lambda_{n+1}, \beta_{long}) \quad (10a)$$

$$\nabla_{a_{CV,n}} H_n(\mathbf{x}_{long,n}, a_{CV,n}, \lambda_{n+1}, \beta_{long}) = 0 \quad (10b)$$

where λ_n is the co-state of $\mathbf{x}_{long,n}$ and the Hamilton's function H_n is defined as follows:

$$H_n(\mathbf{x}_{long,n}, a_{CV,n}, \lambda_{n+1}, \beta_{long}) = \beta_{long}^T L_{long,n}(\mathbf{x}_{long,n}, a_{CV,n}) + \lambda_{n+1}^T (A_n \mathbf{x}_n + B_n u_{EV,n} + C_n u_{CV,n}) \quad (11)$$

In the context of the parameter identification problem, the goal is not to obtain the optimal solution via equations (10a) and (10b), but is described as: given the optimal solution (the real-time collected trajectory data of CV), a set of parameters β_{long} is searched for enabling the trajectory data to best satisfy the necessary condition. Substituting equation (11) into equation (10a), the following equation could be derived:

$$\lambda_{n+1} = (A_n^T)^{-1} \lambda_n - (A_n^T)^{-1} \beta_{long} \nabla_{\mathbf{x}_{long,n}} L_{long,n} \quad (12a)$$

$$= -(A_n^T)^{-1} \nabla_{\mathbf{x}_{long,n}} L_{long,n} (A_n^T)^{-1} \gamma_n \quad (12a)$$

$$\gamma_n = (\beta_{long}, \lambda_n)^T \quad (12b)$$

then the following recursion could be obtained:

$$\gamma_{n+1} = K_n \gamma_n \quad (13a)$$

$$K_n = \begin{pmatrix} I & \mathbf{0} \\ -(A_n^T)^{-1} \nabla_{\mathbf{x}_{long,n}} L_{long,n} & (A_n^T)^{-1} \end{pmatrix} \quad (13b)$$

$$\gamma_{n+1} = K_n K_{n-1} K_{n-2} \dots K_0 \gamma_0 = \mathcal{K}_n \gamma_0 \quad (13c)$$

$$\gamma_0 = (\beta_{long}, \lambda_0)^T \quad (13d)$$

where I denotes identity matrix and $\mathbf{0}$ denotes null matrix. Substituting equation (11) into equation (10b), the following equation could be derived:

$$(\nabla_{a_{CV,n}} L_{long,n} \quad C_{n+1}^T) \gamma_{n+1} = \mathcal{L}_n \gamma_{n+1} = 0 \quad (14)$$

substituting equation (13c) into (14), the following linear equation could be derived:

$$\mathcal{L}_n \mathcal{K}_n \gamma_0 = 0 \quad (15)$$

Thus, the longitudinal driving style parameters β_{long} of CV can be identified by satisfying the equation (15). The lateral driving style parameters β_{lat} follow the same derivation process as β_{long} .

3) Solution method and online implementation

This subsection will introduce the solution method of β and the online implementation scheme. The solution method and the online implementation scheme is suitable for both β_{long} and β_{lat} . This research takes β_{long} as an example in follows.

Due to the noise disturbance or the modeling error, it is difficult to find a set of parameters enabling the collected trajectory data to strictly satisfy equation (15). Based on this fact, the equation (15) could be transformed to the following iterative least-squares optimization problem:

$$\begin{aligned} & \min_{\boldsymbol{\gamma}_0} \sum_n \|\mathcal{L}_n \mathcal{K}_n \boldsymbol{\gamma}_0\|^2 \\ & = \min_{\boldsymbol{\gamma}_0} \boldsymbol{\gamma}_0^T \left(\sum_n (\mathcal{L}_n \mathcal{K}_n)^T (\mathcal{L}_n \mathcal{K}_n) \right) \boldsymbol{\gamma}_0 \\ & = \min_{\boldsymbol{\gamma}_0} \boldsymbol{\gamma}_0^T \mathcal{P}_n \boldsymbol{\gamma}_0 \quad (16) \\ & \text{s.t. } \boldsymbol{e} \boldsymbol{\gamma}_0 = \beta_1 = i \quad (17) \end{aligned}$$

where \mathcal{P}_n is a positive semidefinite matrix; $\boldsymbol{e} = (1,0,0, \dots, 0)$; i is a scaling factor to let the first component of $\boldsymbol{\gamma}_0$ equal to i . Based on the Lagrange multiplier method, the following equation could be obtained:

$$2\mathcal{P}_n \boldsymbol{\gamma}_0 + p \boldsymbol{e}^T = \mathbf{0} \quad (18)$$

β_{long} can be derived from $\boldsymbol{\gamma}_0$ by solving equation (18). Furthermore, [33] have succinctly proven that with the increase of n , $\boldsymbol{\gamma}_0$ definitely converges to a finite value. The algorithm for identifying individual driving styles are summarized as the online implementation scheme illustrated in Figure 4. This algorithm is implemented in an iterative way. At each step, EV collects the real-time trajectory data of CV online and calculates β_{long}^* . Upon β_{long}^* has converged, the algorithm outputs the optimal parameters and terminates.

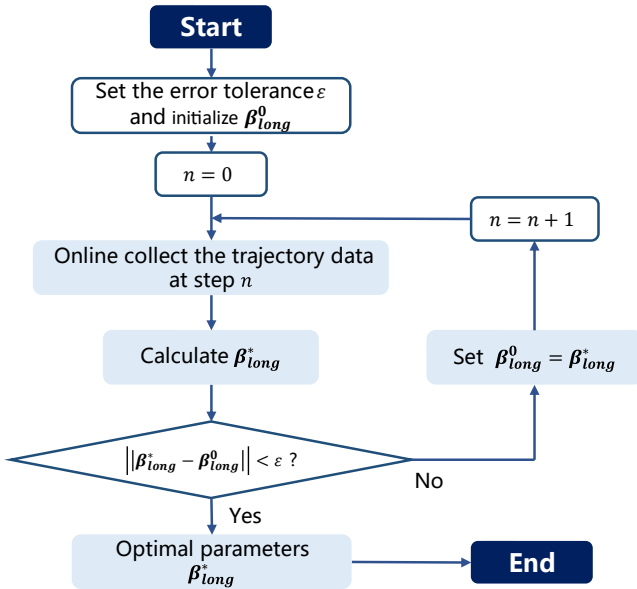


Figure 4 Online implementation scheme of the IOC algorithm.

E. Planner design based on Stackelberg competition

This research designed a Game-based Model Predictive Control (GMPC) planner for the right-of-way protection of EV. Stackelberg competition is adopted as the game rule [35]. Known as a kind of non-cooperative game, Stackelberg competition is a leader-follower game in which the leader takes action first, and the follower reacts to the leader's action based on observations. For this research, EV could be accounted as a leader and proactively compete with the adjacent CV for right-of-way protection; as a follower, CV would react to EV's action.

Figure 5 illustrates the implementation details of the Stackelberg-competition-based planner framework. In the CV

reaction estimation module, this approach assumes that CV follows an optimal control scheme and the optimal reaction can be obtained by solving the Linear Quadratic Regulator (LQR) problem by dynamic programming. In GMPC planner module, this approach utilizes the optimal reaction function of CV to build the EV-CV interaction system dynamics constraint and optimizes commands of control input for EV. After obtaining the control input, EV, as the leader, takes action first (action ① in Figure 5 (III)). Then, CV, as the follower, conducts a reaction (action ② in Figure 5 (IV)), completing the interactive cycle between the leader and the follower in the Stackelberg game context. Finally, the whole process runs to the next time step to update β .

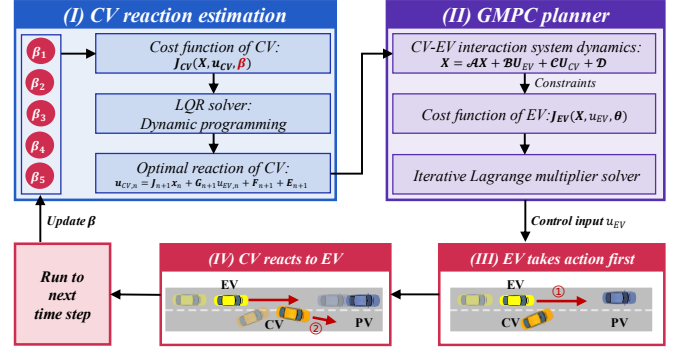


Figure 5 Illustration of Stackelberg-competition-based planner implementation framework.

1) CV reaction estimation

Based on the Stackelberg game framework, CV, as the follower, moves according to its observation on EV. It means that CV can obtain information about EV's current action $u_{EV,n}$. This research assumes that the reaction of CV follows an optimal control scheme and can be obtained by solving the following optimal control problem. The objective is transformed from equation (8):

$$\min_{\boldsymbol{u}_{CV,n} |_{k=0}^{N-1}} (J_{CV}) = \min_{\boldsymbol{u}_{CV,n} |_{n=0}^{N-1}} \left(\sum_{n=0}^{N-1} \frac{1}{2} \left[(\boldsymbol{x}_n - \boldsymbol{x}_{des}^{CV})^T \boldsymbol{Q}_{CV} (\boldsymbol{x}_n - \boldsymbol{x}_{des}^{CV}) + \boldsymbol{u}_{CV,n}^T \boldsymbol{\beta}_d \boldsymbol{u}_{CV,n} \right] \right) \quad (19)$$

where,

$$\boldsymbol{Q}_{CV} = \text{diag}(\beta_1, 0, \beta_2, \beta_4, \beta_5) \quad (20a)$$

$$\boldsymbol{x}_{des}^{CV} = (\Delta \boldsymbol{x}_{des}^{CV}, 0, v_{des}^{CV}, y_{des}^{CV}, \psi_{des}^{CV})^T \quad (20b)$$

$$\boldsymbol{x}_n = \boldsymbol{A}_{n-1} \boldsymbol{x}_{n-1} + \boldsymbol{B}_{n-1} u_{EV,n-1} + \boldsymbol{C}_{n-1} \boldsymbol{u}_{CV,n-1} \quad (20c)$$

$$\boldsymbol{\beta}_d = \text{diag}(\beta_3, 0) \quad (20d)$$

It can be found that \boldsymbol{Q}_{CV} and $\boldsymbol{\beta}_d$ are from the identified driving style β . This optimization problem could be solved by the dynamic programming algorithm. The cost-to-go function is defined as:

$$V(\boldsymbol{x}_i) = \min_{\boldsymbol{u}_{CV,n} |_{n=i}^{N-1}} \left(\sum_{n=i}^{N-1} \frac{1}{2} \left[(\boldsymbol{x}_n - \boldsymbol{x}_{des}^{CV})^T \boldsymbol{Q}_{CV} (\boldsymbol{x}_n - \boldsymbol{x}_{des}^{CV}) + \boldsymbol{u}_{CV,n}^T \boldsymbol{\beta}_d \boldsymbol{u}_{CV,n} \right] + V(\boldsymbol{x}_n) \right) \quad (21a)$$

$$V(\boldsymbol{x}_N) = \frac{1}{2} (\boldsymbol{x}_N - \boldsymbol{x}_{des}^{CV})^T \boldsymbol{M}_N (\boldsymbol{x}_N - \boldsymbol{x}_{des}^{CV}) + \boldsymbol{O}_N^T \boldsymbol{x}_N \quad (21b)$$

where $\boldsymbol{O}_N = (0,0,0,0,0)^T$, $\boldsymbol{M}_N = \text{diag}(0,0,0,0,0)$, and $V(\boldsymbol{x}_N) = 0$. Based on Bellman's optimality principle, the

solution to equation (19) can be achieved via iteratively optimizing this cost-to-go function $V(\mathbf{x}_i)$ in reverse order. Based on the algorithm developed by this research team[21], the optimal control law, also the reaction estimation of CV can be achieved:

$$\mathbf{u}_{CV,n} = \mathbf{J}_{n+1}\mathbf{x}_n + \mathbf{G}_{n+1}u_{EV,n} + \mathbf{F}_{n+1} + \mathbf{E}_{n+1} \quad (n = 0, \dots, N-1) \quad (22)$$

where,

$$\mathbf{J}_{n+1} = -(\mathbf{C}_n^T \mathbf{M}_{n+1} \mathbf{C}_n + \beta_d)^{-1} \mathbf{C}_n^T \mathbf{M}_{n+1} \mathbf{A}_n \quad (23a)$$

$$\mathbf{G}_{n+1} = -(\mathbf{C}_n^T \mathbf{M}_{n+1} \mathbf{C}_n + \beta_d)^{-1} \mathbf{C}_n^T \mathbf{M}_{n+1} \mathbf{B}_n \quad (23b)$$

$$\mathbf{F}_{n+1} = -(\mathbf{C}_n^T \mathbf{M}_{n+1} \mathbf{C}_n + \beta_d)^{-1} \mathbf{C}_n^T \mathbf{M}_{n+1} \mathbf{x}_{des}^{CV} \quad (23c)$$

$$\mathbf{E}_{n+1} = -(\mathbf{C}_n^T \mathbf{M}_{n+1} \mathbf{C}_n + \beta_d)^{-1} \mathbf{C}_n^T \mathbf{M}_{n+1} \mathbf{x}_{des}^{CV} \quad (23d)$$

$\mathbf{M}_n, \mathbf{O}_n$ could be obtained according to $\mathbf{M}_N, \mathbf{O}_N$ and the following recursions in reverse order:

$$\mathbf{O}_n = \mathbf{A}_n^T (\mathbf{I} - \mathbf{C}_n (\mathbf{C}_n^T \mathbf{M}_{n+1} \mathbf{C}_n + \beta_d)^{-1} \mathbf{C}_n^T \mathbf{M}_{n+1})^T (\mathbf{O}_{n+1} + \mathbf{M}_{n+1} \mathbf{B}_n u_{EV,n}) \quad (24)$$

$$\mathbf{M}_n = \mathbf{A}_n^T \mathbf{M}_{n+1} \mathbf{A}_n + \mathbf{Q}_{CV} + \mathbf{A}_n^T \mathbf{M}_{n+1} \mathbf{C}_n (\mathbf{C}_n^T \mathbf{M}_{n+1} \mathbf{C}_n + \beta_d)^{-1} \mathbf{C}_n^T \mathbf{M}_{n+1} \mathbf{A}_n \quad (25)$$

To sum up, in equation (22), the reaction $\mathbf{u}_{CV,n}$ of CV can be estimated according to system state vector \mathbf{x}_n and control input of $u_{EV,n}$. This derivation process is consistent with the assumption of Stackelberg competition framework that the follower reacts to the actions of EV.

2) GMPC planner design

The GMPC planner is designed for EV to protect right-of-way. The reward function \mathcal{R} in POMDP framework is defined as EV's cost function:

$$J_{EV} = \frac{1}{2} \sum_{n=0}^{N-1} \left[\underbrace{\theta_1 (\Delta x - \Delta x_{des}^{EV})^2}_{\text{driving safety}} + \underbrace{\theta_2 (v_{EV} - v_{des}^{EV})^2}_{\text{travel efficiency}} + \underbrace{\theta_3 a_{EV}^2}_{\text{ride comfort}} \right] \quad (26)$$

where Δx_{des}^{EV} represents the desired longitudinal safe distance of EV while v_{des}^{EV} represents the desired speed of EV. The first term in the integral denotes EV's driving safety feature; The second term denotes the mobility feature; The last term mainly specifies ride comfort. $\theta_1, \theta_2, \theta_3$ are weighting factors of each term according to EV users' preference.

The planner is solved in a receding horizon fashion via MPC. According to Stackelberg game rule, CV's reaction formulated in equation (22) is considered in the EV-CV interaction system dynamics constraint.

Cost function formulation: the cost function converts equation (26) into the quadratic programming form:

$$J_{EV} = \frac{1}{2} (\mathbf{X}^T \quad \mathbf{U}_{EV}^T) \mathcal{M} \begin{pmatrix} \mathbf{X} \\ \mathbf{U}_{EV} \end{pmatrix} + \mathbf{q}^T \begin{pmatrix} \mathbf{X} \\ \mathbf{U}_{EV} \end{pmatrix} \quad (27)$$

where:

$$\mathbf{X} = (\mathbf{x}_0, \mathbf{x}_1, \dots, \mathbf{x}_N)^T \quad (28a)$$

$$\mathbf{U}_{EV} = (u_{EV,0}, u_{EV,1}, \dots, u_{EV,N-1})^T \quad (28b)$$

$$\mathcal{M} = \text{diag} \left(\underbrace{\mathbf{Q}_{EV}, \dots, \mathbf{Q}_{EV}}_N, \mathbf{0}_{5 \times 5}, \underbrace{\theta_3, \dots, \theta_3}_N \right) \quad (28c)$$

$$\mathbf{Q}_{EV} = \text{diag}(\theta_1, \theta_2, 0, 0, 0) \quad (28d)$$

$$\mathbf{q} = \left(\underbrace{-\mathbf{Q}_{EV} \mathbf{x}_{des}^{EV}, \dots, -\mathbf{Q}_{EV} \mathbf{x}_{des}^{EV}}_N, 0, \dots, 0 \right)^T \quad (28e)$$

$$\mathbf{x}_{des}^{EV} = (\Delta x_{des}^{EV}, v_{des}^{EV}, 0, 0, 0)^T \quad (28f)$$

EV-CV interaction system dynamics constraint formulation: the EV-CV interaction system dynamics constraint of EV can be transformed from equation (5):

$$\mathbf{X} = \mathbf{A}\mathbf{X} + \mathbf{B}\mathbf{U}_{EV} + \mathbf{C}\mathbf{U}_{CV} + \mathbf{D} \quad (29)$$

where,

$$\mathbf{A} = \begin{bmatrix} \mathbf{0} & \mathbf{0} & \dots & \mathbf{0} & \mathbf{0} \\ \mathbf{A}_0 & \mathbf{0} & \dots & \mathbf{0} & \mathbf{0} \\ \mathbf{0} & \ddots & \ddots & \vdots & \vdots \\ \vdots & \mathbf{0} & \ddots & \mathbf{0} & \vdots \\ \mathbf{0} & \mathbf{0} & \dots & \mathbf{A}_{N-1} & \mathbf{0} \end{bmatrix} \quad (30a)$$

$$\mathbf{B} = \begin{bmatrix} \mathbf{0} & \mathbf{0} & \dots & \mathbf{0} \\ \mathbf{B}_0 & \mathbf{0} & \dots & \mathbf{0} \\ \mathbf{0} & \ddots & \ddots & \vdots \\ \vdots & \mathbf{0} & \ddots & \mathbf{0} \\ \mathbf{0} & \mathbf{0} & \dots & \mathbf{B}_{N-1} \end{bmatrix} \quad (30b)$$

$$\mathbf{C} = \begin{bmatrix} \mathbf{0} & \mathbf{0} & \dots & \mathbf{0} \\ \mathbf{C}_0 & \mathbf{0} & \dots & \mathbf{0} \\ \mathbf{0} & \ddots & \ddots & \vdots \\ \vdots & \mathbf{0} & \ddots & \mathbf{0} \\ \mathbf{0} & \mathbf{0} & \dots & \mathbf{C}_{N-1} \end{bmatrix} \quad (30c)$$

$$\mathbf{D} = (\mathbf{x}_0, 0, \dots, 0)^T \quad (30d)$$

$$\mathbf{U}_{CV} = (\mathbf{u}_{CV,0}, \mathbf{u}_{CV,1}, \dots, \mathbf{u}_{CV,N-1})^T \quad (30e)$$

substituting equation (22) to equation (30e), \mathbf{U}_{CV} can be represented as:

$$\mathbf{U}_{CV} = \mathbf{J}\mathbf{X} + (\mathbf{G} + \mathbf{E})\mathbf{U}_{EV} + \mathbf{F} \quad (31)$$

where,

$$\mathbf{J} = \begin{bmatrix} \mathbf{0} & \mathbf{0} & \dots & \mathbf{0} & \mathbf{0} \\ \mathbf{J}_1 & \mathbf{0} & \dots & \mathbf{0} & \mathbf{0} \\ \mathbf{0} & \ddots & \ddots & \vdots & \vdots \\ \vdots & \mathbf{0} & \ddots & \mathbf{0} & \vdots \\ \mathbf{0} & \mathbf{0} & \dots & \mathbf{J}_N & \mathbf{0} \end{bmatrix} \quad (32a)$$

$$\mathbf{G} = \text{diag}(\mathbf{G}_1, \mathbf{G}_2, \dots, \mathbf{G}_N) \quad (32b)$$

$$\mathbf{F} = \text{diag}(\mathbf{F}_1, \mathbf{F}_2, \dots, \mathbf{F}_N) \quad (32c)$$

$$\mathbf{E} = \begin{bmatrix} \mathbf{0}_{(N-1) \times 2} & \tilde{\mathbf{E}} \\ \mathbf{0}_{1 \times 2} & \mathbf{0}_{1 \times 2(N-1)} \end{bmatrix} \quad (32d)$$

$$\tilde{\mathbf{E}}_{nj} = \begin{cases} -(\mathbf{C}_{n-1}^T \mathbf{M}_n \mathbf{C}_{n-1} + \beta_d)^{-1} \mathbf{C}_{n-1}^T \prod_{i=n+1}^j \mathbf{S}_i \mathbf{T}_{j+1}, & n < j \\ -(\mathbf{C}_{n-1}^T \mathbf{M}_n \mathbf{C}_{n-1} + \beta_d)^{-1} \mathbf{C}_{n-1}^T \mathbf{T}_{n+1}, & n = j \\ \mathbf{0}_{1 \times 2}, & n < j \end{cases} \quad (32e)$$

$$\mathbf{S}_{n+1} = \mathbf{A}_n^T (\mathbf{I} - \mathbf{C}_n (\mathbf{C}_n^T \mathbf{M}_{n+1} \mathbf{C}_n + \beta_d)^{-1} \mathbf{C}_n^T \mathbf{M}_{n+1})^T \quad (32f)$$

$$\mathbf{T}_{n+1} = \mathbf{S}_{n+1} \mathbf{M}_{n+1} \mathbf{B}_n \quad (32g)$$

then, substitute equation (31) to equation (29), the EV-CV interaction system dynamics constraint of EV can be expressed as:

$$(\mathbf{I} - (\mathbf{A} + \mathbf{C}\mathbf{J}) \quad -\mathbf{C}(\mathbf{G} + \mathbf{E}) - \mathbf{B}) \begin{pmatrix} \mathbf{X} \\ \mathbf{U}_{EV} \end{pmatrix} = \mathbf{C}\mathbf{F} + \mathbf{D} \quad (33)$$

To this end, by denoting \mathbf{U}_{CV} by \mathbf{U}_{EV} , the EV-CV

interaction system dynamics constraint is only about \mathbf{U}_{EV} .

Control input constraint: The control input u_{EV} is constrained between a reasonable value range:

$$\mathbf{U}_{min} \leq \mathbf{U}_{EV} \leq \mathbf{U}_{max} \quad (34)$$

where,

$$\mathbf{U}_{max} = \underbrace{(a_{max}, a_{max}, \dots, a_{max})^T}_N \quad (35a)$$

$$\mathbf{U}_{min} = \underbrace{(a_{min}, a_{min}, \dots, a_{min})^T}_N \quad (35b)$$

where a_{max} and a_{min} are the upper and lower boundaries of the control input.

Initial condition constraint: The initial condition is specified as follows:

$$\mathbf{x}_0 = (\Delta x_0, v_{EV}^0, v_{CV}^0, y_{CV}^0, \psi_{CV}^0)^T \quad (36)$$

where the information on the initial condition is collected via sensors and the GPS device of EV.

Speed limit constraint: The speed limit constrains the longitudinal speed of EV. The longitudinal speed shall never exceed the road speed limit while shall be greater than zero:

$$\mathbf{V}_{min} \leq \mathcal{J}\mathbf{U}_{EV} \leq \mathbf{V}_{max} \quad (37)$$

where,

$$\mathbf{V}_{min} = \underbrace{(-v_{EV}^0, -v_{EV}^0, \dots, -v_{EV}^0)^T}_N \quad (38a)$$

$$\mathbf{V}_{max} = \underbrace{(v_{lim} - v_{EV}^0, v_{lim} - v_{EV}^0, \dots, v_{lim} - v_{EV}^0)^T}_N \quad (38b)$$

$$\mathcal{J} = \begin{bmatrix} \Delta t & 0 & \dots & 0 & 0 \\ \Delta t & \Delta t & \dots & 0 & 0 \\ \Delta t & \ddots & \ddots & \vdots & \vdots \\ \vdots & \Delta t & \ddots & \Delta t & 0 \\ \Delta t & \Delta t & \dots & \Delta t & \Delta t \end{bmatrix} \quad (38c)$$

v_{lim} denotes the speed limit of the road; \mathcal{J} is a lower triangular matrix; Δt denotes the length of each time step.

Solution method: according to the cost function equation (27), the EV-CV interaction system dynamics constraint equation (33), and other constraints equation (34) (36) (37), the optimization problem of the GMPC planner is easy to be solved by any quadratic programming algorithm. This research solves the problem by utilizing the iterative Lagrange multiplier method [36] which is proven to be efficient.

IV. EVALUATION

The proposed anti-bullying adaptive cruise control (AACC) approach is assessed and evaluated based on the following aspects: i) ‘‘road-bullying’’ (cut-ins) prevention capability; ii) different CV driving styles adaptation validation; iii) travel efficiency and safety validation; iv) computational efficiency validation. The evaluation contains two parts: function validation and traffic simulation.

A. Experiment design

In this section, the experiment design for the performance evaluation is in detail introduced, including driving style

definition, control types for comparison, and parameter settings.

1) Driving styles definition

In order to demonstrate that the proposed approach is adaptive to different driving styles, CVs with different driving styles are considered. This research categorized the driving styles of CVs into two categories: conservative and aggressive. This research simulates the longitudinal and lateral behavior of different driving styles using the Intelligent Driver Model (IDM) [37] and Minimizing Overall Braking Induced by Lane-change (MOBIL) model [38]. By tuning the parameters of IDM and MOBIL, the driving styles are defined as follows:

- **Conservative:** drivers with a conservative driving style pay more attention to safety and comfort performances rather than efficiency. For IDM, the tuned parameters are: maximum acceleration $a_{max}^{con} = 1m/s^2$, comfortable braking deceleration $b_{com}^{con} = 2m/s^2$, desired time gap $h_{con} = 2.5s$, desired speed $v_{des}^{CV} = 18m/s$; and the parameters for MOBIL are: politeness factor $p_{con} = 0.2$, and lane-changing decision threshold at $a_{th}^{con} = 0.4m/s^2$.
- **Aggressive:** driving requirements of the aggressive drivers are the opposite of conservative drivers. The IDM parameters are: $a_{max}^{agg} = 2.5m/s^2$, $b_{com}^{agg} = 3m/s^2$, $h_{agg} = 0.8s$, and $v_{des}^{CV} = 25m/s$; and for MOBIL: $p_{agg} = 0.05$ and $a_{th}^{agg} = 0.2m/s^2$.

2) Control types for comparison

In this experiment, the performance of the proposed approach is evaluated using two control types:

- **Proposed AACC approach:** in this case, EV is able to online identify the individual driving style of its CV, thus utilizing GMPC planner to proactively protect the right-of-way.
- **Baseline traditional ACC approach:** it is a traditional ACC approach and is unable to proactively protect the right-of-way. It always chooses to decelerate and yield when being cut in. The algorithm is borrowed from [39].

3) Parameter settings

The following settings are adopted for the experiment evaluation:

- The length of the freeway is 3 km.
- Lane width is 3.5m.
- Time step is 0.1 s.
- Optimization horizon is 1 s.
- The speed limit is 25 m/s.
- The acceleration range is $[-3.5, 4] m/s^2$.
- The desired speed of EV and CV is 18m/s.
- The desired longitudinal safe distance of CV is 25 m.
- The desired longitudinal safe distance of EV is 0 m when identifying CV as conservative and 25 m when aggressive.
- Weighting factors $\theta_1, \theta_2, \theta_3$ is 10, 10, and 1 respectively.
- l_r and l_f are both 2 m.

B. Function validation

1) Preparation

Testbed: The function validation platform is Prescan and Matlab/Simulink. A freeway with two lanes is adopted as the testbed to evaluate the performance of the proposed approach. As detailed in Section III-A, EV competes with CV for right-of-way protection. The autonomous driving simulation software PreScan is used to generate the scenario and control EV. The proposed approach is coded with Matlab/Simulink. The control modules of CV and PV are also coded in Matlab/Simulink. Through communication of PreScan and Matlab/Simulink, the test for the proposed approach can be implemented. Figure 6 explicitly depicts the structure of the testbed.

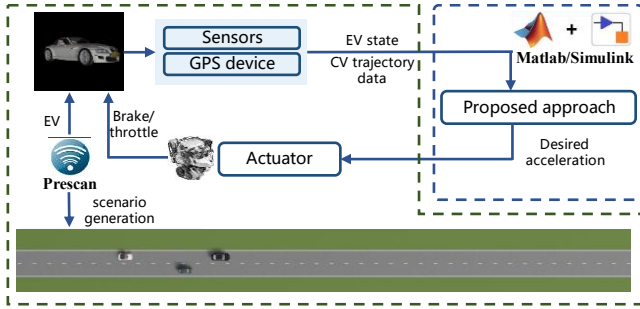


Figure 6 The structure of the testbed in function validation.

Sensitive analysis: Sensitivity analysis considers two factors: driving styles and the initial longitudinal distance between EV and CV. Conservative and aggressive driving styles of CVs are all tested. The initial longitudinal distance between EV and CV contains 10m, 20m, and 30m. It is used to measure the capability of proactively right-of-way protection.

Metrics: The following metrics are utilized for performance evaluation:

- Speed, longitudinal position, and sampled trajectories of EV and CV are used to validate right-of-way protection capability.
- The identified driving style parameters of CV are used for different CV driving styles adaptive validation.
- The average speed of EV is used to measure the mobility advantage of the proposed approach.
- The time-integrated time headway (TTH) of EV is adopted to quantitatively verify the safety improvement of the proposed approach [40]. It is defined as the integration of time headway values of EV below the time headway safety threshold for a period of time. The lower TTH value means the safer performance. Figure 7 explicitly depicts the definition of the TTH of EV. The time headway safety threshold is set as 1.5 s.

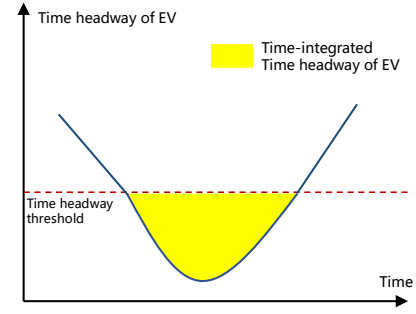


Figure 7 Illustration of time-integrated time headway of EV.

2) Main results

The function validation results demonstrate that the proposed AACC approach: i) is capable of preventing cut-ins, thus proactively protecting right-of-way; ii) is adaptive to different driving styles of CV; iii) has benefits in travel efficiency enhancement by up to 29.55%; iv) has better safety performance by relieving the aggravation of potential risks.

Right-of-way protection capability: The proposed approach is proven to have right-of-way protection capability as shown in Figure 8 and Figure 9, in which two scenarios corresponding to two different driving styles of CVs are selected out.

Figure 8 presents the validation results when CV with a conservative style. In this scenario, the proposed approach proactively protects the right-of-way of EV by leaving no room for CV to cut in. To be detailed, EV decisively accelerates to overtake and CV reacts to EV's accelerating behavior by decelerating and yielding as shown in Figure 8 (a) and (b). Figure 8 (c) shows that CV chooses to cut in behind EV.

Figure 9 presents the validation results when CV with an aggressive style. In this scenario, the proposed approach lowers the safety risk by yielding to CV. To be detailed, EV decelerates when CV aggressively speeds up and cuts in. It can be seen that EV abandons the overtaking maneuver and decelerates to widen the gap from the aggressive CV in Figure 9 (a) and (b). Figure 9 (c) shows that EV waits for CV to cut in.

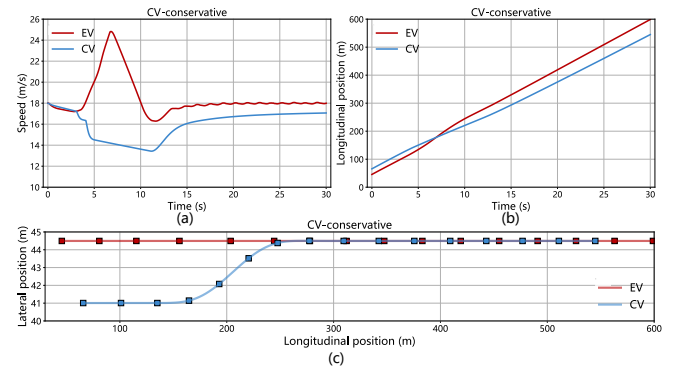


Figure 8 Validation results when CV is with a conservative style: (a) speed; (b) longitudinal position; (c) sampled trajectories. (The mark points denote the vehicles' position every 2 seconds)

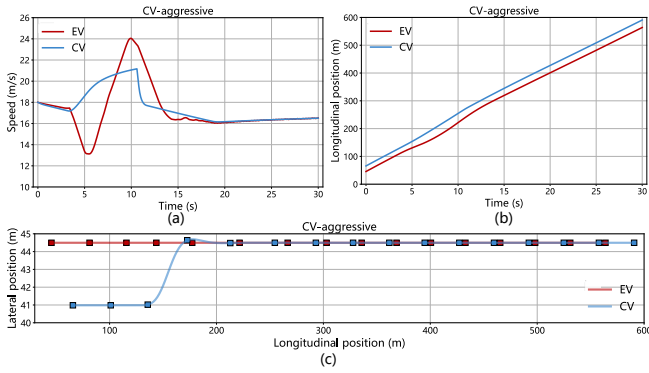


Figure 9 Validation results when CV is with an aggressive style: (a) speed; (b) longitudinal position; (c) sampled trajectories. (The mark points denote the vehicles' position every 2 seconds)

Different CV driving styles adaptive validation: TABLE 1 shows the driving style identification results corresponding to scenarios in Figure 8 and Figure 9. The results confirm that the proposed approach can be adaptive to different driving styles of CVs. By giving the individual driving style of CV, the proposed approach can make case-specific decisions. As illustrated in TABLE 1, β_2 of the conservative CV is far smaller than the aggressive CV which means the conservative CV has less desire for travel efficiency. β_3 and β_5 of the conservative CV are larger than the aggressive CV which means the aggressive CV has a higher travel efficiency desire over safety and comfort compared with the conservative CV.

TABLE 1 The results of the identified driving style parameters.

Driving style parameter	CV-conservative	CV-aggressive
β_1	1	1
β_2	0.00139	3.540
β_3	0.873	0.657
β_4	1	1
β_5	0.132	0.101

Travel efficiency quantification: The travel efficiency of the proposed approach is quantified by the average speed in Figure 10 (a) and Figure 11 (a). Results in Figure 10 (a) show that the proposed approach outperforms and has benefits in travel efficiency improvement by up to 29.55% when faced with a conservative CV compared with the baseline traditional ACC. A sensitive analysis of different cut-in gaps demonstrates that the average speed of the proposed approach increases with CV's cut-in gaps. It makes sense that EV has to accelerate longer to overtake CV when CV's cut-in gaps increase. However, the proposed approach has no obvious travel efficiency improvement when faced with an aggressive CV, as shown in Figure 11 (a). The rationale behind this is that the proposed approach identifies the aggressive driving style of CV and conducts deceleration.

Safety performance quantification: The safety performance of the proposed approach is quantified by TTH in Figure 10 (b) and Figure 11 (b). Results in Figure 10 (b) show that the proposed approach has better safety performance under 10m and 20m cut-in gaps compared with the baseline traditional ACC. The TTH benefits are 79.8% and 62.2% respectively. That's because the proposed approach can

predictively overtake CV to avoid smaller time headway values due to being behind CV. However, under 30m cut-in gaps, the proposed approach has worse safety performance than the baseline traditional ACC. The sensitive analysis demonstrates that the safety performance of the proposed approach decreases with CV's cut-in gaps. That's because the overtaking process is riskier as the cut-in gap is longer. Results in Figure 11 (b) show that the proposed approach has better safety performance across all cut-in gaps. The proposed approach has significant safety enhancement by up to 0.9 s² THT reduction. The reason is that the proposed approach can predictively decelerate to avoid smaller time headway values when faced with the aggressive CV.

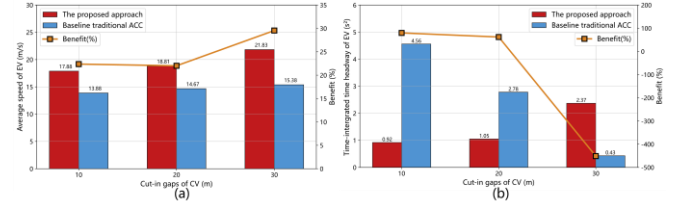


Figure 10 Validation results under different cut-in gaps when CV is with a conservative style: (a) average speed of EV; (b) safety level of EV.

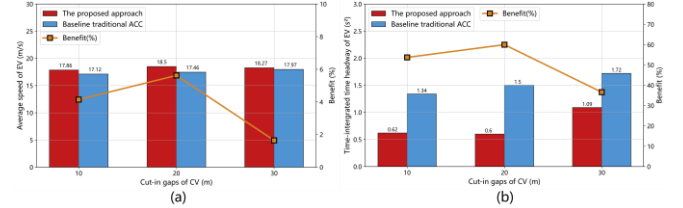


Figure 11 Validation results under different cut-in gaps when CV is with an aggressive style: (a) average speed of EV; (b) safety level of EV.

C. Simulation in the context of traffic

1) Preparation

Testbed: The traffic simulation platform is PTV Vissim and Matlab/Simulink. The traffic simulation software PTV Vissim is used to build a 3 km two-lane-freeway and generate background traffic flow with different driving styles. It also provides an API named COM for Matlab/Simulink to control EV. Figure 12 explicitly depicts the structure of the testbed.

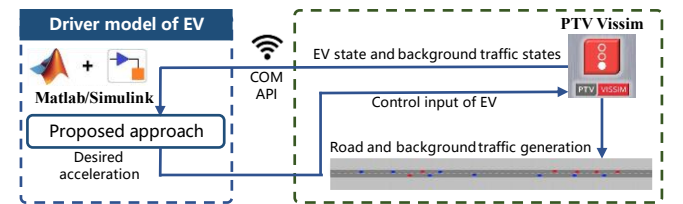


Figure 12 The structure of the testbed in traffic simulation.

Sensitive analysis: Sensitivity analysis is about congestion levels. Four congestion levels are tested: $v/c=0.2$; $v/c=0.4$; $v/c=0.6$; $v/c=0.8$. It is expected the proposed approach would have different performance under different congestion levels. The v/c ratio greater than or equal to 1 is not considered. That's because vehicles have difficulty executing cut-ins in oversaturated traffic conditions. Each congestion level would be simulated ten times randomly.

Metrics: The following metrics are utilized for performance evaluation:

- The travel time of EV is used to measure the travel efficiency in traffic flow. It is defined as the average time spent during traveling the same distance.
- Speed standard deviation of EV is used to evaluate the robustness of the adaptive cruising performance.
- Computation time is used to evaluate the computational efficiency of the proposed approach.
- Time headway distribution of EV is adopted to evaluate the safety and flexibility of the proposed approach. This research set 10.5 s as the upper bound of vehicles' time headway.

2) Main results

The traffic simulation results demonstrate that the proposed AACC approach: i) reduces travel time in traffic flow by up to 11.93%; ii) improves speed robustness by 8.74% on average; iii) adopts more flexible and competitive driving strategies; iv) supports field implementation by ensuring a 50 milliseconds computation time.

Travel efficiency in traffic flow: The travel efficiency is evaluated by the travel time, as illustrated in Figure 13. Results show that the proposed approach achieves maximum travel time reduction by 11.93%, compared with baseline traditional ACC. A sensitive analysis is conducted in terms of different v/c ratios. Travel time for both the baseline and the proposed approach increases with increasing v/c ratio. It can be seen the proposed approach spent lower travel time in all v/c ratios. The rationale behind it is that the proposed approach can proactively protect the right-of-way and avoid being obstructed by cut-in vehicles. However, the benefit of the proposed approach decreases with v/c ratios from 0.4 to 0.6. That's because the driving space is more sufficient in a v/c ratio of 0.4, so the proposed approach can maintain more mobility when preventing some cut-ins. Moreover, the benefit in the v/c ratio of 0.8 is the highest. The reason is that the proposed approach can overtake more cut-in vehicles to obtain more travel efficiency.

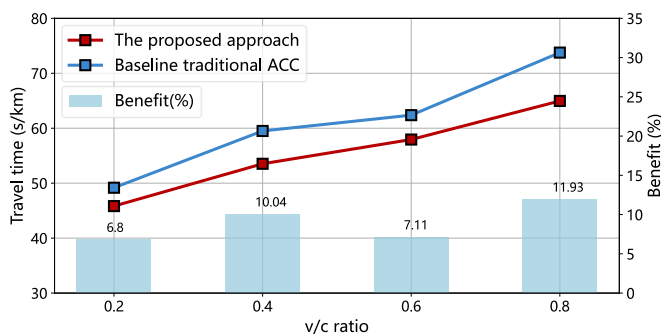


Figure 13 Comparison of EV's travel time under different v/c ratios.

Travel robustness in traffic flow: The travel robustness is assessed by the speed standard deviation of EV as shown in TABLE 2. Results show that the speed standard deviation improvement is 8.74% on average. The proposed approach has a benefit in speed standard deviation by 18.23% at maximum. A sensitive analysis is conducted in terms of different v/c ratios. It can be seen that in v/c ratios of 0.4, 0.6, and 0.8, the proposed approach has a smaller mean speed standard deviation than the baseline. The reason is that the proposed approach can predictively react to cut-in vehicles

avoiding drastic speed fluctuations. However, it's noteworthy that the proposed approach has a slightly larger mean speed standard deviation in the v/c ratio of 0.2. This is due to the fact that cut-ins are reduced at low congestion levels and the demand for the proposed approach is reduced.

TABLE 2 Comparison of EV's speed standard deviation under different v/c ratios.

Control types	Speed standard deviation of EV (m/s)			
	v/c=0.2	v/c=0.4	v/c=0.6	v/c=0.8
Proposed approach	4.69	5.93	5.00	5.83
Traditional ACC	4.60	6.57	5.49	7.13
Benefit (%)	-1.96%	9.74%	8.93%	18.23%

Computational efficiency: The proposed approach supports online field implementation through computation time quantification, as illustrated in Figure 14. Results reveal that the average computation time is 9.54 milliseconds across all settings. A sensitive analysis is conducted in terms of planning horizons and planning steps. Results show that the computation time increases with increasing planning horizons and decreasing planning steps. The proposed AACC approach can ensure a 50-millisecond computation time in nearly all cases.

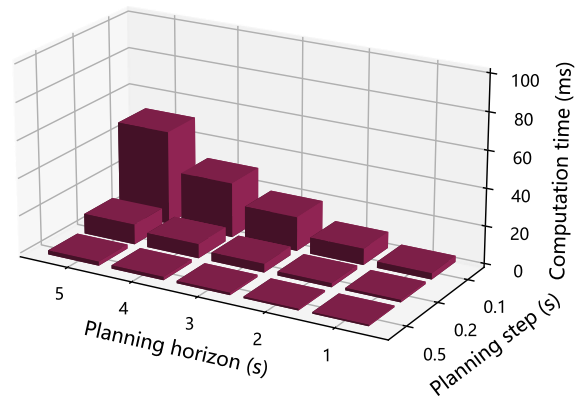


Figure 14 The computation time regarding varying parameter settings.

Travel flexibility in traffic flow: The proposed approach allows for more flexible and competitive strategies, as illustrated in Figure 15. A sensitive analysis is conducted in terms of different v/c ratios. In a v/c ratio of 0.2, the proposed approach has a larger average time headway which means better safety performance. That's because in uncongested traffic, right-of-way protection can avoid being obstructed, hence avoiding small time headways. In v/c ratios more than 0.2, the proposed approach has a slightly smaller average time headway than the baseline traditional ACC. The rationale behind this is that the driving behavior of the proposed approach is more aggressive and competitive. The proposed approach often accelerates to prevent mandatory cut-ins. Moreover, In v/c ratios more than 0.2, the peak of the distribution density of the proposed approach is smaller and the distribution is more uniform. In contrast, the distribution of the baseline is more centralized than that of the proposed approach. The reason is that the baseline can only keep the artificially designed safe distance to the preceding vehicles. While the proposed approach can adopt more flexible and competitive driving strategies according to the situation and other vehicles' driving styles.

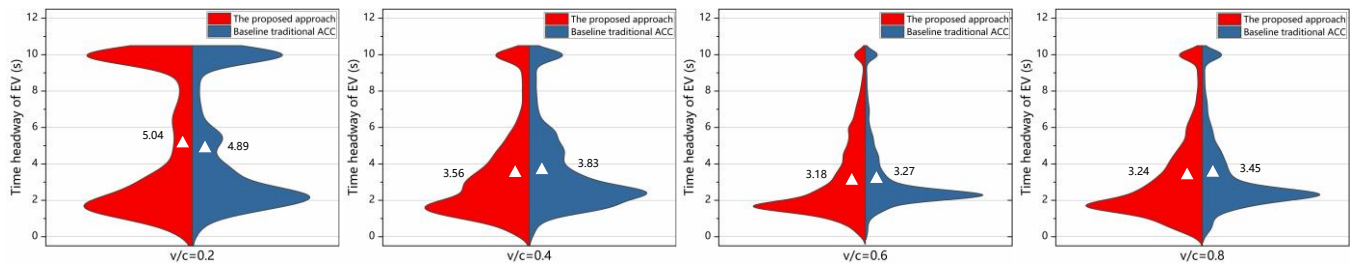


Figure 15 Comparison of EV's time headway distribution under different v/c ratios.

V. CONCLUSION

This research proposed an Anti-bullying Adaptive Cruise Control (AACC) approach. It bears the following features: i) with the enhanced capability of preventing bullying from cut-ins; ii) optimal but not unsafe; iii) adaptive to various driving styles of the opponent cut-in vehicle; iv) with real-time field implementation capability. To realize the proactive right-of-way protection capability, a Game-based Model Predictive Control (GMPC) planner is designed, and Stackelberg competition is adopted as the game rule. An online Inverse Optimal Control (IOC) algorithm is leveraged to identify the individual driving behavior of the competing vehicles in order to enable person-by-person countermeasures. The problem is solved by a highly efficient quadratic programming algorithm. To evaluate the proposed approach, simulation experiments were conducted. The results have shown that:

- The proposed approach can prevent bullying from cut-ins which means the ego vehicle protects its right-of-way.
- The proposed approach is adaptive to different competing vehicles' driving styles by optimizing the driving strategy in person-by-person manners.
- The proposed approach is capable of enhancing travel efficiency by up to 29.55% under different cut-in gaps.
- The proposed approach can strengthen driving safety in most cases. However, in cases of the largest cut-in gaps, the proposed approach cannot enhance safety performance.
- The proposed approach is efficient and robust against traffic congestion levels. It can reduce mean travel time by up to 11.93% and reduce mean speed standard deviation by 8.74% on average.
- The proposed approach can adopt more flexible and competitive driving strategies as the time headway distribution results show.
- The proposed approach can ensure less than 50 milliseconds of computation time across all parameter settings.

Although the proposed approach has achieved many benefits, it still has some limitations. For example, the proposed approach lacks the consideration of cooperative driving. Therefore, future research could be conducted on the joint optimization of the EV and CV's motions which might further improve traffic efficiency and safety. In addition, it needs to be pointed out that the proposed approach does not consider the stochasticity of human

driver behavior. Further work could consider enhancing the proposed approach with greater robustness.

REFERENCES

- [1] M. Makridis, K. Mattas, A. Anesiadou, and B. Ciuffo, "OpenACC. An open database of car-following experiments to study the properties of commercial ACC systems," *Transportation Research Part C: Emerging Technologies*, vol. 125, p. 103047, 2021/04/01/2021, doi: <https://doi.org/10.1016/j.trc.2021.103047>.
- [2] L. Xiao and F. Gao, "A comprehensive review of the development of adaptive cruise control systems," *Vehicle System Dynamics*, vol. 48, no. 10, pp. 1167-1192, 2010, doi: [10.1080/00423110903365910](https://doi.org/10.1080/00423110903365910).
- [3] L. Yu and R. Wang, "Researches on Adaptive Cruise Control system: A state of the art review," *Proceedings of the Institution of Mechanical Engineers, Part D: Journal of Automobile Engineering*, vol. 236, no. 2-3, pp. 211-240, 2022, doi: [10.1177/09544070211019254](https://doi.org/10.1177/09544070211019254).
- [4] G. Lu, J. Zhai, P. Li, F. Chen, and L. Liang, "Measuring drivers' takeover performance in varying levels of automation: Considering the influence of cognitive secondary task," *Transportation Research Part F: Traffic Psychology and Behaviour*, vol. 82, pp. 96-110, 2021/10/01/2021, doi: <https://doi.org/10.1016/j.trf.2021.08.005>.
- [5] Y. Zhang, Y. Lin, Y. Qin, M. Dong, L. Gao, and E. Hashemi, "A New Adaptive Cruise Control Considering Crash Avoidance for Intelligent Vehicle," *IEEE Transactions on Industrial Electronics*, vol. 71, no. 1, pp. 688-696, 2024, doi: [10.1109/tie.2023.3239878](https://doi.org/10.1109/tie.2023.3239878).
- [6] M. Mirabilio, A. Iovine, E. De Santis, M. D. D. Benedetto, and G. Pola, "A Mesoscopic Human-Inspired Adaptive Cruise Control for Eco-Driving," *IEEE Transactions on Intelligent Transportation Systems*, vol. 24, no. 9, pp. 9571-9583, 2023, doi: [10.1109/tits.2023.3275706](https://doi.org/10.1109/tits.2023.3275706).
- [7] S. Lapardhaja, Y. Gong, M. Tausif Murshed, and X. David Kan, "Commercial Adaptive Cruise Control (ACC) and Capacity Drop at Freeway Bottlenecks," *International Journal of Transportation Science and Technology*, 2024, doi: [10.1016/j.ijst.2024.07.011](https://doi.org/10.1016/j.ijst.2024.07.011).
- [8] G. Zhang, Z. Wang, B. Fan, L. Zhao, and Y. Qi, "Adaptive cruise control system with traffic jam tracking function based on multi-sensors and the driving behavior of skilled drivers," *Advances in Mechanical Engineering*, vol. 10, no. 9, 2018, doi: [10.1177/1687814018795801](https://doi.org/10.1177/1687814018795801).
- [9] M. Jaswanth, N. K. L. Narayana, S. Rahul, and M. Supriya, "Autonomous Car Controller using Behaviour Planning based on Finite State Machine," in *2022 6th International Conference on Trends in Electronics and Informatics (ICOEI)*, 28-30 April 2022 2022, pp. 296-302, doi: [10.1109/ICOEI53556.2022.9776684](https://doi.org/10.1109/ICOEI53556.2022.9776684).
- [10] T. Salzmann, B. Ivanovic, P. Chakravarty, and M. Pavone, "Trajectron++: Dynamically-Feasible Trajectory Forecasting with Heterogeneous Data," in *Computer Vision – ECCV 2020*, Cham, A. Vedaldi, H. Bischof, T. Brox, and J.-M. Frahm, Eds., 2020/2020: Springer International Publishing, pp. 683-700.
- [11] Z. Huang, H. Liu, J. Wu, and C. Lv, "Conditional Predictive Behavior Planning With Inverse Reinforcement Learning for Human-Like Autonomous Driving," *IEEE Transactions on Intelligent Transportation Systems*, vol. 24, no. 7, pp. 7244-7258, 2023, doi: [10.1109/TITS.2023.3254579](https://doi.org/10.1109/TITS.2023.3254579).
- [12] Z. Huang, H. Liu, J. Wu, W. Huang, and C. Lv, "Learning Interaction-aware Motion Prediction Model for Decision-making in Autonomous Driving," *arXiv preprint arXiv:2302.03939*, 2023.

- [13] C. Tang, W. Zhan, and M. Tomizuka, "Interventional Behavior Prediction: Avoiding Overly Confident Anticipation in Interactive Prediction," in 2022 IEEE/RSJ International Conference on Intelligent Robots and Systems (IROS), 23-27 Oct. 2022 2022, pp. 11409-11415, doi: 10.1109/IROS47612.2022.9981524.
- [14] B. Gao, K. Cai, T. Qu, Y. Hu, and H. Chen, "Personalized Adaptive Cruise Control Based on Online Driving Style Recognition Technology and Model Predictive Control," IEEE Transactions on Vehicular Technology, vol. 69, no. 11, pp. 12482-12496, 2020, doi: 10.1109/tvt.2020.3020335.
- [15] Li, Y., 2017. Deep Reinforcement Learning: an Overview arXiv preprint arXiv: 1701.07274.
- [16] J. Hu, S. Li, H. Wang, Z. Wang, and M. J. Barth, "Eco-approach at an isolated actuated signalized intersection: Aware of the passing time window," Journal of Cleaner Production, vol. 435, 2024, doi: 10.1016/j.jclepro.2023.140493.
- [17] V. Bhattacharyya and A. Vahidi, "Automated Vehicle Highway Merging: Motion Planning via Adaptive Interactive Mixed-Integer MPC," in 2023 American Control Conference (ACC), 31 May-2 June 2023 2023, pp. 1141-1146, doi: 10.23919/ACC55779.2023.10156567.
- [18] D. Li, A. Liu, H. Pan, and W. Chen, "Safe, Efficient and Socially-Compatible Decision of Automated Vehicles: A Case Study of Unsignalized Intersection Driving," Automotive Innovation, vol. 6, no. 2, pp. 281-296, 2023/05/01 2023, doi: 10.1007/s42154-023-00219-2.
- [19] G. Lu, Y. Nie, X. Liu, and D. Li, "Trajectory-based traffic management inside an autonomous vehicle zone," Transportation Research Part B: Methodological, vol. 120, pp. 76-98, 2019/02/01/ 2019, doi: <https://doi.org/10.1016/j.trb.2018.12.012>.
- [20] C. Wei, Y. He, H. Tian, and Y. Lv, "Game Theoretic Merging Behavior Control for Autonomous Vehicle at Highway On-Ramp," IEEE Transactions on Intelligent Transportation Systems, vol. 23, no. 11, pp. 21127-21136, 2022, doi: 10.1109/TITS.2022.3174659.
- [21] Z. Zhang, X. Yan, H. Wang, C. Ding, L. Xiong, and J. Hu, "No more road bullying: An integrated behavioral and motion planner with proactive right-of-way acquisition capability," Transportation Research Part C: Emerging Technologies, vol. 156, p. 104363, 2023/11/01/ 2023, doi: <https://doi.org/10.1016/j.trc.2023.104363>.
- [22] G. Markkula et al., "Defining interactions: a conceptual framework for understanding interactive behaviour in human and automated road traffic," Theoretical Issues in Ergonomics Science, vol. 21, no. 6, pp. 728-752, 2020/11/01 2020, doi: 10.1080/1463922X.2020.1736686.
- [23] N. Bao, A. Carballo, and T. Kazuya, "Prediction of Personalized Driving Behaviors via Driver-Adaptive Deep Generative Models," in 2021 IEEE Intelligent Vehicles Symposium (IV), 11-17 July 2021 2021, pp. 616-621, doi: 10.1109/IV48863.2021.9575671.
- [24] X. Tang et al., "Prediction-Uncertainty-Aware Decision-Making for Autonomous Vehicles," IEEE Transactions on Intelligent Vehicles, vol. 7, no. 4, pp. 849-862, 2022, doi: 10.1109/TIV.2022.3188662.
- [25] Z. Huang, J. Wu, and C. Lv, "Driving Behavior Modeling Using Naturalistic Human Driving Data With Inverse Reinforcement Learning," IEEE Transactions on Intelligent Transportation Systems, vol. 23, no. 8, pp. 10239-10251, 2022, doi: 10.1109/tits.2021.3088935.
- [26] B. Zhu, S. Yan, J. Zhao, and W. Deng, "Personalized Lane-Change Assistance System With Driver Behavior Identification," IEEE Transactions on Vehicular Technology, vol. 67, no. 11, pp. 10293-10306, 2018, doi: 10.1109/TVT.2018.2867541.
- [27] Z. Gu et al., "Integrated eco-driving automation of intelligent vehicles in multi-lane scenario via model-accelerated reinforcement learning," Transportation Research Part C: Emerging Technologies, vol. 144, p. 103863, 2022/11/01/ 2022, doi: <https://doi.org/10.1016/j.trc.2022.103863>.
- [28] Y. Huang, J. Du, Z. Yang, Z. Zhou, L. Zhang, and H. Chen, "A Survey on Trajectory-Prediction Methods for Autonomous Driving," IEEE Transactions on Intelligent Vehicles, vol. 7, no. 3, pp. 652-674, 2022, doi: 10.1109/TIV.2022.3167103.
- [29] H. Deng, Y. Zhao, Q. Wang, and A.-T. Nguyen, "Deep Reinforcement Learning Based Decision-Making Strategy of Autonomous Vehicle in Highway Uncertain Driving Environments," Automotive Innovation, vol. 6, no. 3, pp. 438-452, 2023/08/01 2023, doi: 10.1007/s42154-023-00231-6.
- [30] W. Liu, S.-W. Kim, S. Pendleton, and M. H. Ang, "Situation-aware decision making for autonomous driving on urban road using online POMDP," in 2015 IEEE Intelligent Vehicles Symposium (IV), 2015: IEEE, pp. 1126-1133.
- [31] H. Wang, W. Hao, J. So, Z. Chen, and J. Hu, "A Faster Cooperative Lane Change Controller Enabled by Formulating in Spatial Domain," IEEE Transactions on Intelligent Vehicles, vol. 8, no. 12, pp. 4685-4695, 2023, doi: 10.1109/TIV.2023.3317957.
- [32] R. Rajamani, "Lateral Vehicle Dynamics," in Vehicle Dynamics and Control, R. Rajamani Ed. Boston, MA: Springer US, 2012, pp. 15-46.
- [33] T. L. Molloy, J. J. Ford, and T. Perez, "Online inverse optimal control for control-constrained discrete-time systems on finite and infinite horizons," Automatica, vol. 120, p. 109109, 2020/10/01/ 2020, doi: <https://doi.org/10.1016/j.automatica.2020.109109>.
- [34] N. Kim, S. Cha, and H. Peng, "Optimal Control of Hybrid Electric Vehicles Based on Pontryagin's Minimum Principle," IEEE Transactions on Control Systems Technology, vol. 19, no. 5, pp. 1279-1287, 2011, doi: 10.1109/TCST.2010.2061232.
- [35] F. Etro, "Stackelberg Competition with Endogenous Entry," The Economic Journal, vol. 118, no. 532, pp. 1670-1697, 2008, doi: 10.1111/j.1468-0297.2008.02185.x.
- [36] H. Wang, J. Lai, X. Zhang, Y. Zhou, S. Li, and J. Hu, "Make space to change lane: A cooperative adaptive cruise control lane change controller," Transportation Research Part C: Emerging Technologies, vol. 143, p. 103847, 2022/10/01/ 2022, doi: <https://doi.org/10.1016/j.trc.2022.103847>.
- [37] M. Liebner, M. Baumann, F. Klanner, and C. Stiller, "Driver intent inference at urban intersections using the intelligent driver model," in 2012 IEEE Intelligent Vehicles Symposium, 3-7 June 2012 2012, pp. 1162-1167, doi: 10.1109/IVS.2012.6232131.
- [38] A. Kesting, M. Treiber, and D. Helbing, "General Lane-Changing Model MOBIL for Car-Following Models," Transportation Research Record, vol. 1999, no. 1, pp. 86-94, 2007/01/01 2007, doi: 10.3141/1999-10.
- [39] M. Zhu, Y. Wang, Z. Pu, J. Hu, X. Wang, and R. Ke, "Safe, efficient, and comfortable velocity control based on reinforcement learning for autonomous driving," Transportation Research Part C: Emerging Technologies, vol. 117, p. 102662, 2020/08/01/ 2020, doi: <https://doi.org/10.1016/j.trc.2020.102662>.
- [40] G. F. B. Piccinini, C. M. Rodrigues, M. Leitão, and A. Simões, "Driver's behavioral adaptation to Adaptive Cruise Control (ACC): The case of speed and time headway," Journal of safety research, vol. 49, pp. 77. e1-84, 2014.